Biomaterials 29 (2008) 3983–3992

Contents lists available at ScienceDirect

Biomaterials

journal homepage: www.elsevier.com/locate/biomaterials

The effect of platelet-rich plasma on healing in critical-size long-bone defects

Philip Kasten [a,*], Julia Vogel [a], Florian Geiger [c], Philipp Niemeyer [b], Reto Luginbühl [d], Krisztian Szalay [a]

[a] Orthopaedic Surgery Hospital, University of Heidelberg, Schlierbacher Landstrasse 200a, 69118 Heidelberg, Germany
[b] Department of Orthopaedics and Traumatology, University of Freiburg, Freiburg, Germany
[c] Department of Orthopaedic Surgery, University of Frankfurt, Frankfurt, Germany
[d] Dr. h.c. Robert Mathys Foundation, Bettlach, Switzerland

ARTICLE INFO

Article history:
Received 6 April 2008
Accepted 13 June 2008
Available online 9 July 2008

Keywords:
Platelet
Stem cell
Bone regeneration
Bone tissue engineering
Bone healing
Calcium phosphate

ABSTRACT

The role of platelet-rich plasma (PRP) as a promoter of bone healing remains controversial. The hypothesis investigated was that PRP improves bone healing of a critical-size diaphyseal radius defect in a rabbit model. The bone defect was filled with a high-surface ceramic scaffold, calcium-deficient hydroxyapatite (CDHA), with the addition of allogenic PRP, mesenchymal stem cells (MSC) or both. PRP yielded better bone formation than the empty CDHA scaffold as determined by both histology and micro-computer tomography ($p < 0.05$) after 16 weeks, whereas no difference was observed on biomechanical testing. Similar behavior was found in samples with MSC; however, the combination of MSC and PRP did not further improve bone healing. Furthermore, the resorption of CDHA was improved by the addition of PRP, MSC and MSC/PRP, but there were no differences between the groups. The areas of bone formation were greater in areas adjacent to the bone resection areas and towards the intact ulna. In conclusion, PRP improves bone healing in a diaphyseal rabbit model on CDHA and the combination of CDHA. This study supports the allogenic use of PRP for bone healing as an off-the-shelf therapy.

1. Introduction

Massive bone defects constitute a major challenge to reconstructive surgery. Autogenous bone grafting is considered the gold standard for filling bone defects even today, despite significant problems arising from donor-site morbidity and limited amount of donor bone [1,2]. Therefore, bone regeneration by means of tissue engineering has attracted increasing interest. The concept of tissue engineering is based on three pillars: (1) scaffolds; (2) cells; and (3) growth factors.

Ceramics are promising materials for tissue engineering because they offer three-dimensional support and serve as a scaffold for cell proliferation, cell differentiation and ultimately for bone formation. A variety of degradable and osteoconductive biomaterials are available and clinically utilized [3,4]. Mostly, synthetic β-tricalcium phosphates (β-TCP) or calcium phosphates from corals are used [4]. A disadvantage of these biomaterials is their low specific surface area (SSA) of less than 1 m^2/g. A new group of resorbable high-SSA ceramics is emerging that has proved to be equally effective regarding osteogenic differentiation in vitro [5] and ectopic bone formation in vivo, e.g., β-TCP [6,7]. Calcium-deficient hydroxyapatite (CDHA) is a member of this high-SSA ceramic group, with a SSA of 20–80 m^2/g, approaching the values of about 80 m^2/g found in natural bone [5]. Cells adhere more easily to high-SSA ceramics, e.g., β-TCP, than to low-SSA scaffolds [5].

To improve their osteogenic potential, scaffolds can be combined with mesenchymal stem cells (MSC) and/or growth factors. MSC are multipotential cells and can differentiate into osteoblasts, chondrocytes, adipocytes, tenocytes, myoblasts or marrow stroma [8]. MSC can be isolated from a bone marrow aspirate and rapidly expanded in vitro. Numerous preclinical studies have shown that MSC expanded in vitro can regenerate critical-size bone defects when combined with bone substitutes [4,9,10]. Growth factors influence the chemotaxis, differentiation, proliferation and synthetic activity of bone cells, thereby regulating physiological remodeling and fracture healing. Numerous growth factors, such as bone morphogenetic proteins (BMPs), platelet-derived growth factor (PDGF), transforming growth factor-β (TGF-β), and insulin-like growth factors (IGF), have a stimulating effect on bone defect healing [11]. Platelet-rich plasma (PRP) contains a number of these growth factors [PDGF, TGF-β1, TGF-β2, IGF, epidermal growth factor (EGF), and epithelial cell growth factor (ECGF)] in its natural composition [12]. Because it can be used autogenously, it poses no risk of transmissible diseases. Furthermore, PRP can easily be obtained on the day of surgery by two centrifugation steps from autogenous whole blood. Basic research seems to endorse PRP's ability to support bone and soft tissue healing [3,13]. Marx et al. used PRP as a source of autogenous thrombocytic growth factors for the

* Corresponding author. Tel.: +49 6221 965; fax: +49 6221 966 347.
E-mail address: Philip.Kasten@ok.uni-heidelberg.de (P. Kasten).

0142-9612/$ – see front matter © 2008 Elsevier Ltd. All rights reserved.
doi:10.1016/j.biomaterials.2008.06.014

reconstruction of maxillofacial defects in humans and found that PRP resulted in quicker maturation of autogenous bone transplants and higher bone density [14]. However, recently there have been conflicting reports about the effect of PRP plasma, and there is no consensus regarding the role of PRP in bone regeneration [15–19].

To our knowledge, there are sparse data on the effect of PRP on the healing of critical-size long-bone defects. This model, however, is of fundamental interest because it comes close to the situation of non-union where the orthopedic surgeon attempts healing by measures other than simply bone grafting and/or internal stabilization. Therefore, we decided to examine the effect of PRP in combination with autogenous MSC and the aforementioned high-SSA scaffold CDHA in a rabbit model. The main outcome parameters were biomechanical stability, newly formed bone and resorption of the ceramic as shown on micro-computer tomography (μ-CT) and histology.

2. Materials and methods

2.1. Animals

Six- to 9-month-old female New Zealand white rabbits (NZWR) were kept in separate cages, fed a standard diet and allowed to move freely during the study. The following groups (each $n = 6$) were compared: the critical-size defect was filled with: (1) a CDHA scaffold and autogenous MSC; (2) CDHA and PRP; or (3) CDHA, autogenous MSC and PRP. As controls served (4) the CDHA scaffold alone; (5) an empty defect; and (6) a defect filled with autogenous cancellous bone from the iliac crest. Animals were treated in compliance with our institution's guiding principles "in the care and use of animals". The local ethics committee for animal experiments approved the design of the experiment. Two animals in the control group with empty defects and one animal in the CDHA + PRP group sustained a fracture of the forearm and were excluded from the study.

2.2. Ceramic scaffolds and PRP

Calcium-deficient hydroxyapatite ceramic cylinders of 15 mm length and 4 mm diameter [Robert Mathys Foundation (RMS), Switzerland] were produced in an emulsion process as described earlier [20,21]. The ceramic had a total porosity of 85 vol%, 54 vol% for macropores (0.2–0.6 mm) and 31 vol% for micropores (<5 μm). Its specific surface area approximated 48 m^2/g. For the preparation of the PRP, on average 17 ml (SD 3.67) of blood was obtained from the ear arteries of six anesthetized 6-month old NZWR. The protocol was adapted from Yamada et al. [19]. The blood was collected in tubes that were rinsed with heparin and the platelets were counted in Neugebauer chambers. The average platelet number was 1.9×10^8 (SD 0.39×10^8)/ml. Then, the blood was centrifuged twice: initially at $209 \times g$ for 16 min at 20 °C to remove red blood cells and then at $1500 \times g$ for 12 min at 20 °C to obtain the platelet pellet. The cell pellet was resuspended in platelet-poor plasma, resulting in an average platelet number of 10.05×10^8/ml (SD 3.2×10^8). The PRP of the six donors was mixed and stored at −80 °C until needed, and consequently allogenic PRP was used.

2.3. Isolation and cultivation of autogenous rabbit mesenchymal stem cells

Two weeks prior to the surgery when the bone defect was created, bone marrow was harvested from all animals. According to a preoperative randomized protocol animals in the autogenous MSC group ($n = 6$) and the autogenous MSC + PRP group ($n = 6$) received their expanded MSC. The surgical technique was the following: with the animal under general anesthesia, the bone marrow of the tibia was penetrated antegrade via the proximal anterior tibial metaphysis using a sterile bone marrow aspiration needle with a diameter of 3 mm. After reaching the marrow space and removing the trocar, the bone marrow was aspirated using a 2-ml syringe containing 0.1 ml heparin. The aspirated marrow was mixed in a 15-ml Falcon tube containing 5 ml of pre-digestion medium [0.5 ml of collagenase (1.5 mg/ml), 0.5 ml of hyaluronidase (1 mg/ml) and 4 ml of Verfaillie medium] [22]. Then, the marrow aspirate was homogenized with a pipette. The aspirate was subsequently left to incubate at 39 °C while spinning at 35 rpm continuously for 8 h (RM 540; CAT, Stauffen, Germany). Once digestion ceased, 10 ml of PBS was added, and the pre-digested marrow aspirate was filtered by use of a 40 μm filter. The samples were washed in phosphate-buffered saline (PBS) (1:2) and centrifuged for 10 min at $677 \times g$. Subsequently, the cells were counted and afterwards plated in cell culture flasks (Easy Flask filter, Nunclon™ surface; Nunc A/S, Roskilde, Denmark) in modified expansion medium according to Verfaillie with the addition of 2% fetal calf serum (FCS) [22]. After 24 h, non-adhesive cells were discarded and adhesive cells were washed once with PBS. Standard culturing conditions were used (37 °C, 6% CO_2), and the medium was changed twice a week. At 80–90% confluence, cells were harvested with trypsin/EDTA (Biochrom, Berlin, Germany), and replated by splitting usually 1:3 at a density of 50–60%. Cells were cultivated until passage 2–4, equaling 16–19 population doublings. The mesenchymal differentiation potential for the osteogenic, chondrogenic and the adipogenic lineage was demonstrated qualitatively in vitro from aliquots of the adherent cells of the bone marrow aspirate as reported previously [23]. Therefore, the cells fulfill the criteria of mesenchymal stem/stromal cells [22].

2.4. Loading of cells and application of PRP

All ceramics were incubated overnight at 4 °C in 40-μM/ml fibronectin (Sigma, Taufkirchen, Germany) solution diluted in PBS to improve the adhesion of the cells and because it was found to be beneficial for bone formation [23]. The cells to be transplanted were detached from the culture flasks by trypsin and counted. Five million cells were then resuspended in 3 ml of culture medium and transferred into a 5-ml tube. The ceramics were placed into the medium containing the cells. After 1.5 h of continuous spinning at 37 °C (35×/min), the ceramics were placed into a six-well plate. The medium containing the cells was centrifuged twice at $800 \times g$ for 5 min, and the resulting cell pellet was resuspended in 70 μl of culture medium and applied to the ceramics. Previous studies demonstrated that loading MSC statically on CDHA had an efficiency of 95% [7]. After loading of the cells the MSC remain in the superficial layers within a depth of 1–2 mm [7]. Forty microliters of freshly thawed PRP was then applied to the ceramics of the PRP group, and subsequently 10 μl thrombin (0.8 IU activity)—calcium chloride (1 M) solution (1:1) (Tissucol-duo; Baxter, Unterschleißheim, Germany) was added directly before implantation. Animals that received PRP had no local inflammatory response, nor systemic immune responses such as fevers were noticed.

2.5. Surgery

The animal model was adapted from Wittbjer et al. as described previously [24,25]. Briefly, unilateral 15-mm critical-size defects were created in the distal radial diaphysis. The rabbits were anesthetized with an intramuscular injection of ketamine hydrochloride (50 mg/kg BW, Hostaket®; Intervet, Tönisvorst, Germany) and xylazine (5 mg/kg BW, Rompun®; Bayer Vital, Leverkusen, Germany). An antibiotic (netilmicin 4 mg/kg BW, Certomycin®; Essex Pharma, Munich, Germany) was administered perioperatively. A superomedial incision of 3 cm was made over the distal radius, soft tissues were dissected, and the bone was exposed by gentle retraction of the muscles. A Hohmann retractor was placed between ulna and radius to protect the ulna. A 15-mm segmental diaphyseal defect was created with an oscillating saw under irrigation with 0.9-vol% sterile saline solution. The periosteum was removed with the bone and 5 mm of periosteum was stripped from each side of the remaining proximal as well as distal main fragment. The defect was irrigated with sterile physiological saline solution, and the ceramic (or cancellous bone, or nothing) was press fitted into the defect. Muscles, fascia and skin were separately closed over the defect with 4-0 resorbable sutures (Ethilon; Ethicon, Norderstedt, Germany). Fixation of the osteotomized radius was unnecessary because of the fibro-osseous union of ulna and radius proximal and distal to the surgical site and the press fit of the implant. In the cancellous bone group, the cancellous bone was harvested through a separate 2-cm incision above the posterior iliac crest. The fascia was divided and the edge of the iliac crest was osteotomized. The cancellous bone was then harvested by use of a curette between the layers of cortical bone. The wound was closed in layers. Postoperatively, 4 mg/kg body weight of carprofen was given as needed for pain. There were no differences in carprofen administration among the groups. Water and food were supplied ad libitum. After 16 weeks the animals were killed. After immediate mechanical testing, the specimens were placed in 70% ethanol.

2.6. Radiographic evaluation

Standardized anteroposterior and lateral radiographs were taken immediately postoperatively and every 4 weeks thereafter to monitor the placement of the graft and the bony integration. An ultra-high-definition film (44 kV and 2.2 mA with a constant X-ray to object to film distance of 171 cm) was used.

2.7. Biomechanical testing procedure

A four point non-destructive bending test was performed immediately after the animal was killed by means of a testing device (type 1387; Zwick, Einsingen/Ulm, Germany) adapted from the model of Mattila et al. and Reddy et al. [26,27]. First, the forearm was exarticulated at the elbow joint. Then, the wrist and the soft tissues of the forearm were carefully dissected to visualize the area of the bone defect without touching the ceramic or the bone. The ulna was loaded at two points, 40 mm apart from each other. The indentor was positioned at the radius and consisted of two parallel points of identical length that were placed 12 mm apart at each side. The radial defect was centered exactly between these two points. Both the loading points and the indentor were round and had a diameter of 2 mm to avoid cutting into the bone when loaded. The test was motion controlled with a speed of 0.08 mm/s. The data were automatically recorded and stored in a desktop computer interfaced with the material testing device. The strain curves (N/mm) were analyzed for the elastic linear deformation zone with exclusion of the plastic deformation zone. From the slope of the linear elastic deformation curve the stiffness (Young's modulus) was

calculated. To account for interindividual differences in bone diameter the stiffness of the operated leg was normalized to the stiffness of the contralateral forearm (in percent). Each contralateral forelimb was measured at the same position as the ipsilateral forelimb.

2.8. Micro-computer tomography

After mechanical testing, the specimens, containing the 1.5-cm segmental defect and 0.5 cm of proximal and 0.5 cm of distal cortical bone adjacent to the defect, were fixed in 70-vol% alcohol. Each bone block was examined with a micro-computer tomography (μ-CT) system (Fanbeam Micro-CT; Stratec, Stuttgart, Germany). The microfocus of the X-ray source of the μ-CT system had a spot size of 7 μm and a maximum voltage of 36 kV. The image matrix was 1024 × 1024 pixels. The specimens were placed in a sample holder filled with water. They were oriented in such a way that the long axis of the block was parallel to the axis of the sample holder. A high-resolution protocol (slice thickness 120 μm, feed 60 μm, pixel size 60 μm) was applied. Depending on the length of the specimens, up to 180 slices was scanned perpendicular to the block. To determine the amount of newly formed bone tissue, the best threshold for the CDHA scaffold alone was selected visually followed by determination of the threshold for the CDHA scaffold and newly formed bone together. In addition, the ranges and means of the gray levels characteristic of the CDHA scaffold and newly formed bone were determined. The CDHA scaffold showed a mean gray level of 160 ± 15, while that of the newly formed bone was 60 ± 15. The visually determined threshold to separate CDHA scaffold from newly formed bone was set at 100, allowing reliable distinction between the two tissue types. Finally, μ-CT slices were compared with the corresponding histological slides to verify the reliability of the discrimination criteria. The digitized data were analyzed with VG Studio Max 1.2.1 software (Volume Graphics, Heidelberg, Germany), and the amount of new bone formation (newly formed bone voxels per complete tissue voxels of the initially implanted CDHA volume) was calculated. Resorption was calculated by dividing the voxels of the ceramic that was present after 16 weeks by the voxels of the mean of three CDHA cylinders that were not implanted.

2.9. Histological analysis

After mechanical testing and μ-CT analysis, the non-decalcified specimens were dehydrated in ascending grades of alcohol and embedded in Technovit (Technovit 7200 VLC; Kulzer GmbH, Wehrheim, Germany). During embedding, the positioning of the radius was standardized in an attempt to ensure that the same region was evaluated in all specimens. Then, 50-μm coronal sections with the radius and ulna parallel were made, using a sawing and grinding technique (Exakt Apparatebau, Hamburg, Germany). From each animal one section was stained with Goldner's trichrome and one with Giemsa and toluidine. The sections were examined using a light microscope (Axioplan 2 Imaging; Zeiss, Göttingen, Germany). The Giemsa/toluidine-stained specimens were digitized and analyzed with the program Image J, National Institutes of Health [28]. The type of tissue was identified manually, marked and assigned to a color. In detail, the areas of newly formed bone, connective tissue and ceramic were calculated per total bone defect area (Fig. 1A). In addition, a 3 × 4-mm area adjacent to the ceramic/bone interface (Fig. 1B) and, in another approach, the half of the radial defect that was next to the ulna were separately evaluated for area of new bone formation (Fig. 1C), i.e. the areas of bone per total area were calculated.

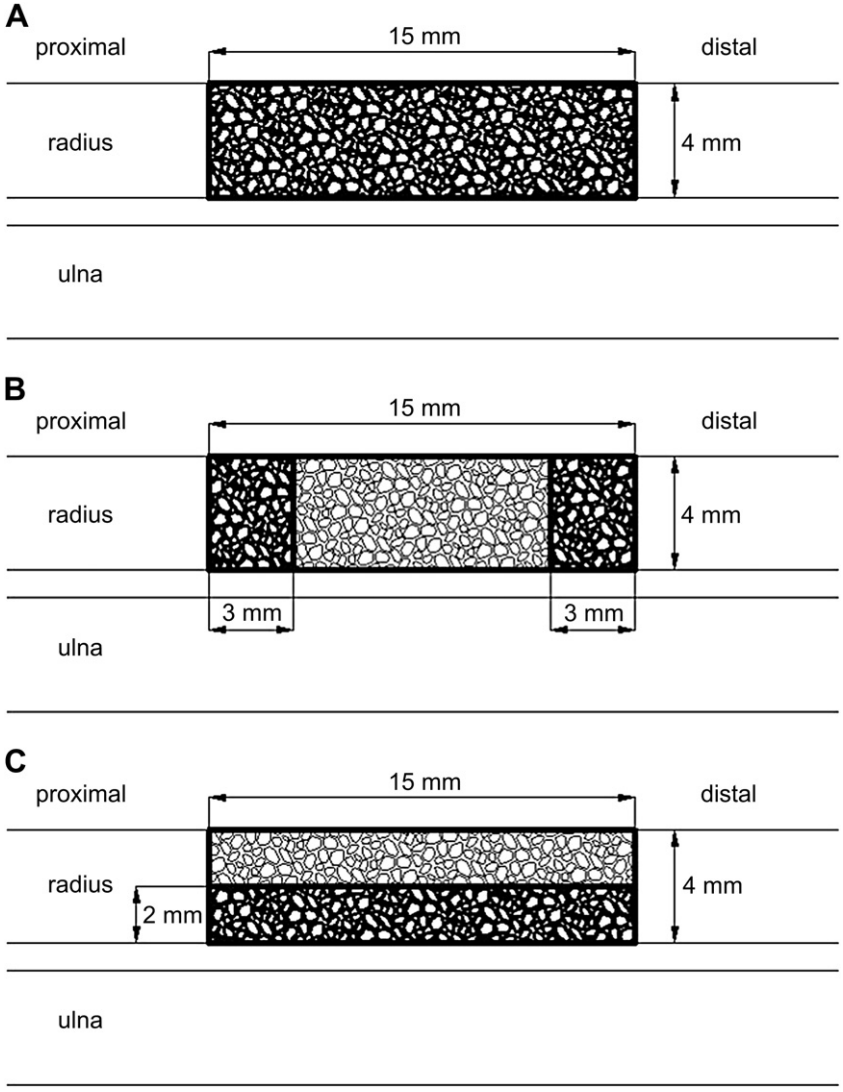

Fig. 1. To examine the effect of adjacent bone on bone formation in histology, distinct regions of interest were defined. (A) The extent of bone formation in the total defect area was measured and normalized to the total defect area. (B) The bone area at the interface to the ceramic at an area 3 × 4 mm was normalized to the total interface area. (C) Bone formation adjacent to the ulna was measured separately.

2.10. Statistical analysis

Data analysis was performed with SPSS for Windows 15.0 (SPSS Inc., Chicago, IL, USA). Mean values and standard deviations were calculated. The main outcome measures were stiffness during the biomechanical testing and newly formed bone and ceramic resorption in μ-CT and histology. These were examined by multifactorial analysis of variance (ANOVA). Differences between the independent variables were checked in post-hoc tests [Tukey's studentized range (HSD) tests for variables]. The alpha error was consequently adjusted. The extent of bone formation at the interface area and the ulnar half of the bony defect were compared to the extent of bone formation in the total defect area with a matched paired Wilcoxon test. *P* values <0.05 were considered significant. All tests were two-tailed.

Data analysis was performed with SPSS for Windows 12.0 (SPSS Inc.).

3. Results

3.1. Biomechanical results

The relative stiffness of the CDHA, CDHA + MSC, CDHA + PRP and CDHA + MSC + PRP groups were significantly higher than in the empty group ($p < 0.05$) (Fig. 2). The autogenous cancellous bone group had significantly higher values than CDHA, CDHA + MSC and CDHA + MSC + PRP ($p < 0.05$), but not than CDHA + PRP (Fig. 2). The differences between CDHA, CDHA + MSC, CDHA + PRP and CDHA + MSC + PRP animals were not statistically significant. All operated forearms revealed lower stiffness than the intact contralateral forearms.

3.2. Bone volume and CDHA ceramic resorption measured in μ-CT

The volume of the newly formed bone in the CDHA + MSC, CDHA + PRP and CDHA + MSC + PRP animals was significantly higher than in the animals that received only CDHA ($p < 0.05$) (Table 1, Figs. 3 and 4). Defects treated with autogenous cancellous bone had regenerated entirely. The new bone formation was minimal in the empty control group, which was not significantly different from the CDHA-only group. There were no differences in the volume of the newly formed bone among the CDHA + PRP, CDHA + MSC and CDHA + MSC + PRP groups. The residual volume of the CDHA scaffold was significantly lower in the CDHA + MSC, CDHA + PRP and CDHA + MSC + PRP animals than in the CDHA animals (Table 2) ($p < 0.05$). There were also no differences in the residual volume of the CDHA scaffold among the CDHA + PRP, CDHA + MSC and CDHA + MSC + PRP groups.

3.3. Histological results

In general, the histological findings were in accordance with the results of μ-CT analysis and the X-rays (Fig. 5). Little or no new bone formed in the empty defects. The autogenous bone transplant integrated with the local bone, proximally and distally. The area of newly formed bone was higher in defects treated with CDHA + MSC and with CDHA + MSC + PRP than in defects treated with CDHA alone ($p < 0.05$) (Fig. 6). This trend did not reach significance comparing the empty defect with the CDHA + PRP group. The ulnar half ($p = 0.0005$) and the interface area ($p = 0.006$) of the bone defect contained significantly more bone than the total defect surface in the CDHA + MSC, CDHA + PRP and CDHA + MSC + PRP groups (Figs. 6 and 7). The histology specimens were examined for the presence of lymphocytes or multinucleated giant cells/macropaghes. There were no differences between the groups. The bone tissue formed in the periphery of the ceramic pores without a fibrous layer between the bone and the ceramic. This indicates that the scaffold has osteoconductive properties. The pores adjacent to the ulna and in the interface towards the radius were even completely filled with bone.

4. Discussion

The hypothesis for this study was that PRP promotes bone healing in a critical-size long-bone defect on calcium-deficient

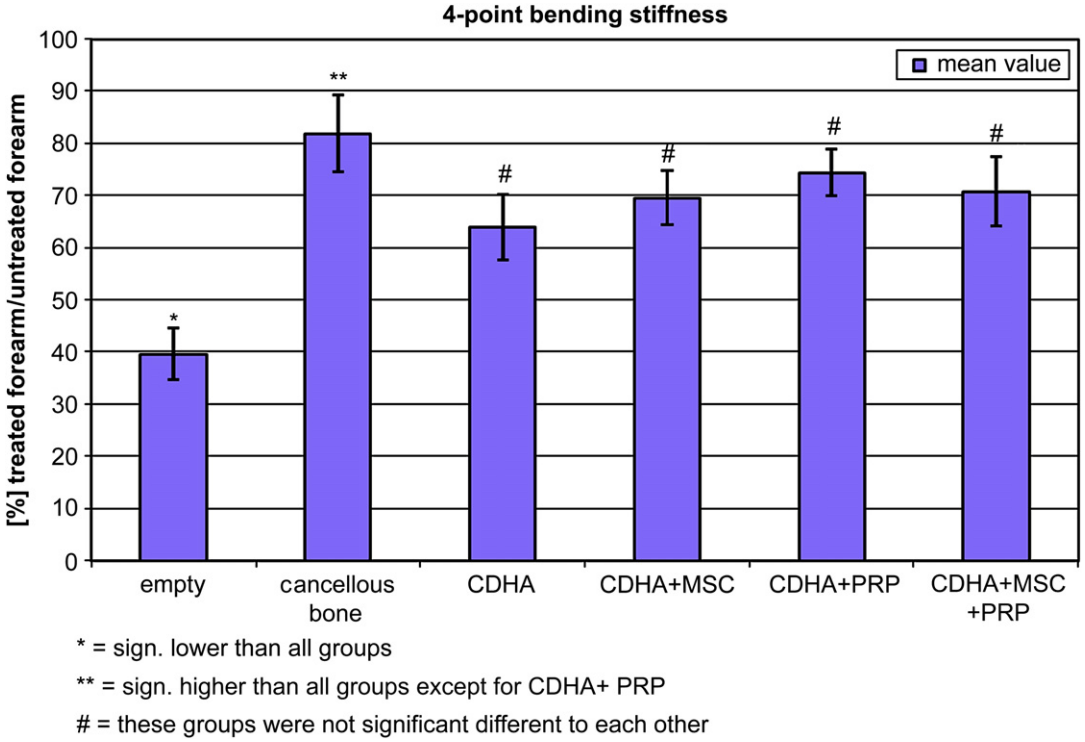

Fig. 2. Implantation of the CDHA scaffold resulted in a higher stiffness than the empty defect in all cases. The cancellous bone group had the highest stiffness of all groups, the difference being significant from all but the CDHA + PRP group. Mean values and SD are presented. The numbers were $n = 4$ in the empty group, $n = 5$ in the CHDA + PRP group and $n = 6$ in the other groups.

Table 1
New bone formation in μ-CT

Independent variable	Subgroup	Mean value ± SD (% of total CDHA cylinder volume)	*n*	Post-hoc comparison[a]	*p* value[b]/df/*z* value
	Empty	4.2 ± 3.9	5	a	<0.0001/6/149.52
	Cancellous bone	92.33 ± 10.42	6	b	
	CDHA only	11 ± 3.58	6	a	
	CDHA + rabbit MSC	22.83 ± 5.98	6	c	
	CDHA + PRP	24.8 ± 5.54	5	c	
	CDHA + rabbit MSC + PRP	26.67 ± 6.28	6	c	

[a] Different letters indicates significant differences between homogeneous subgroups at an alpha level of $p < 0.05$. For example, the empty group (post-hoc comparison, letter a) is significant different to the cancellous bone (letter b), but not to the CDHA only group (letter a).
[b] By ANOVA.

hydroxyapatite (CDHA), a high-surface ceramic scaffold. The data demonstrate that the addition of PRP had a significantly positive effect on bone formation as shown on μ-CT and on histology. The effect was similar to that of MSC on the CDHA scaffold; however, the combination of MSC and PRP had no additional effect.

Basic research endorses the ability of PRP to promote bone healing [13,19,29–32]. In addition, clinical studies have shown that after implanting bone grafts in mandibular bone defects, the bone density and the maturation rate are significantly greater when the grafts are used in combination with PRP than when they are used alone [14,33]. PRP seems to have a positive effect in the early phase of bone healing in combination with autogenous cancellous bone grafts [3,34,35], and in diabetic fracture healing [16]. When mixed with an autogenous bone graft and activated, the PRP forms a gel containing cytokines and growth factors essential for the progression of coordinated wound healing, improved vascularity and tissue regeneration [3,35,36]. In combination with bovine cancellous blocks PRP increased bone formation in a non-critical-size bone defect in rabbit cranium [37].

A critical analysis of other studies shows, however, that a beneficial effect of PRP on bone healing could not be demonstrated in combination with every bone substitution material and every animal model: in goats, the addition of PRP to autogenous cancellous bone did not improve bone healing of a critical-size forehead-bone defect [38]. The addition of PRP to β-tricalcium phosphate (β-TCP) failed to improve bone healing in an anterior spinal fusion [17] and a critical-size forehead defect [3] in pigs. PRP in combination with bovine cancellous blocks had no positive effect in a forehead defect of pigs [3] or in a rat mandible defect [18] and even decreased bone formation around titanium implants in tibia defects in dogs [39]. PRP that was placed around titanium dental implants failed to improve bone healing in the mandibles of dogs [40]. In a non-critical-size rat cranial bone defect, PRP did not improve bone healing on hydroxyapatite/TCP particles [41]. Especially in the later course of bone healing, some authors could not demonstrate positive effects of PRP [3,15,42]. Our group investigated the effect of PRP on different kinds of scaffolds and found a trend towards better performance of PRP in combination with CDHA than with β-TCP in SCID mice after subcutaneous implantation [43]. As a subcutaneous implant cannot be compared to a bone defect, our group proceeded to study the biomaterial CDHA in a long-bone defect in combination with PRP in the study presented here. A critical-size diaphyseal bone defect was chosen because this is more difficult to heal than a metaphyseal defect due to the lower vascularity. Indeed, the untreated empty controls showed no healing at all in the current study.

The high-surface scaffold CDHA has an approximately 100 times higher specific surface area (SSA) than, for example, β-TCP, which

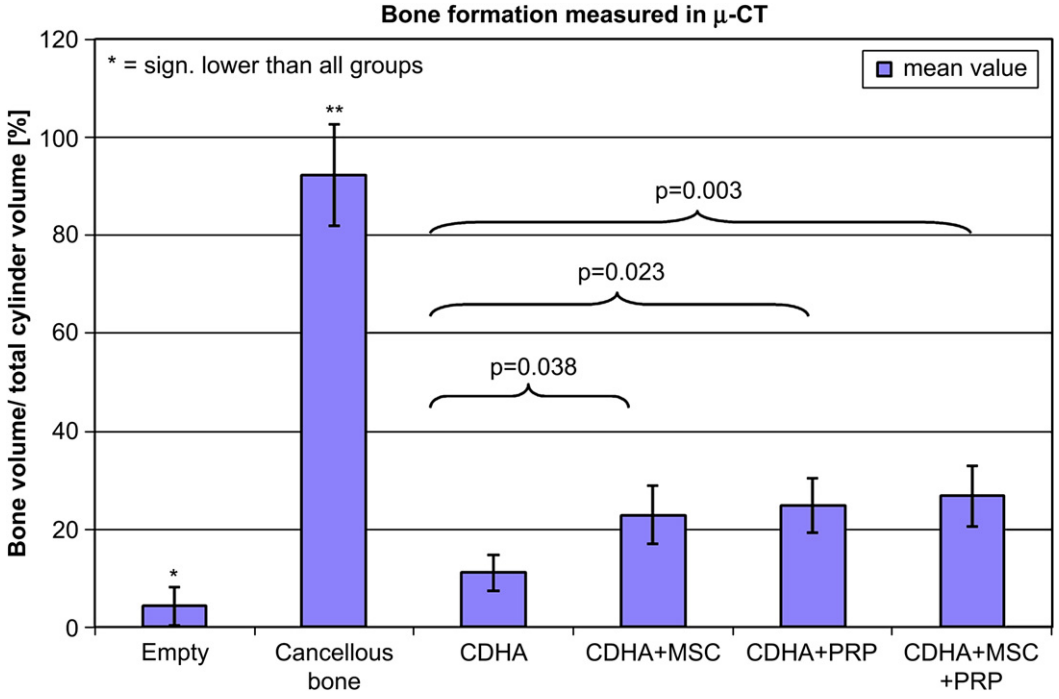

Fig. 3. The addition of MSC and/or PRP resulted in greater bone formation than in the CDHA-only group. There were no significant differences between the CDHA + MSC, CDHA + PRP and CDHA + PRP + MSC groups. The numbers were $n = 4$ in the empty group, $n = 5$ in the CHDA + PRP group and $n = 6$ in the other groups.

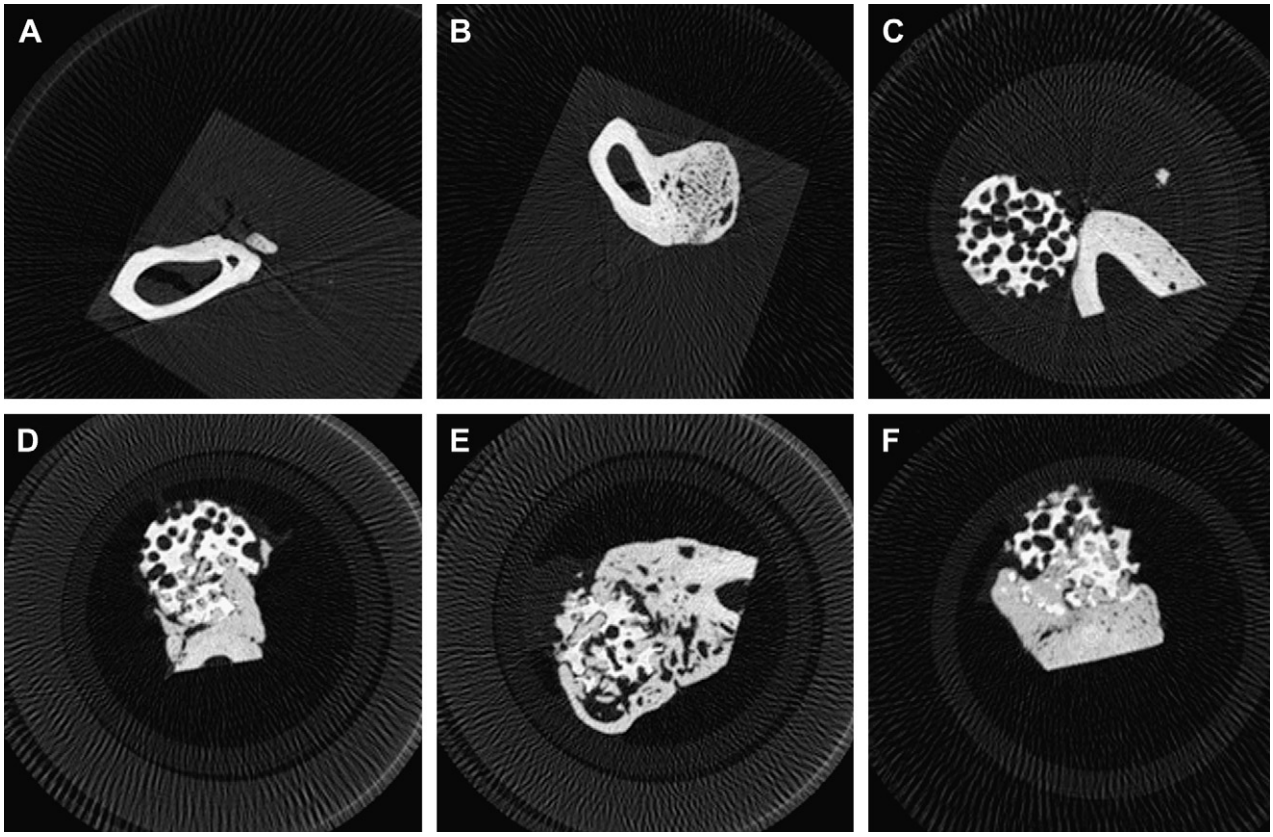

Fig. 4. This set of μ-CT images shows a representative transverse section of the forearm at a standardized position in the middle of the bony defect at 30-μm resolution 16 weeks after implantation. A is the empty defect, B the defect filled with autogenous spongiosa, C the empty CDHA scaffold, D the CDHA with MSC scaffold, E the CDHA with PRP, and F the CDHA with MSC and PRP.

can affect protein adsorption. The high SSA of CDHA may allow more extensive and longer absorption of PRP, and the rough surface of CDHA may cause stronger degranulation and release of the growth factors from the platelets.

An important parameter for the performance of PRP is the method of its preparation, since this can significantly influence the concentrations of platelets and growth factors [44], and consequently their osteogenic capacity [3]. Recommendations for the platelet concentrations in PRP range from three to five times its original concentration in whole blood [14,18]. Higher platelet concentrations do not necessarily correlate with higher levels of growth factors such as TGF-β1 [34]. Furthermore, recently an in vitro study showed that the concentration of growth factors were species dependent, being highest in human PRP, followed by goat and rat PRP [45]. The degranulation of PRP and the release of the growth factors can be achieved by the addition of thrombin in the presence of calcium chloride or by thawing the platelets [14,46]. In an attempt to maximize and standardize the growth factor release, the platelets were both thawed and activated by thrombin and calcium chloride.

In summary, the role of PRP remains controversial. Several studies have shown a positive effect, mainly on early bone healing, while others have not. However, previous studies could hardly be compared because the study designs were very different. Factors that can influence the efficacy of PRP as promoter of bone healing are: the biomaterial, the species, the site of implantation, and the preparation and activation of the PRP.

It is assumed that PRP might support osteogenesis in the presence of precursor cells. However, the addition of PRP could not further increase the rate of bone formation in our model. Obviously, the quantity and composition of the growth factors that are contained in PRP (PDGF, TGF-β1, TGF-β2, IGF, EGF, ECGF) [12] were not able to cause a strong osteogenic effect on the MSC. This might mean that the effect of PRP is weak and PRP of limited use in patients. On the other hand, an explanation could be that the MSC introduced into the defect were already relatively strongly induced towards osteogenesis and PRP could not significantly increase this. Another issue is the injury to the bone due to the osteotomy of the radius: it is known that after a bone injury growth factors and host precursors are released [47]. Maybe this effect was strong enough to stimulate the MSC and it could not be further increased by PRP.

The fact that the addition of allogenic PRP alone without MSC was able to induce bone formation equivalent to the application of MSC might have clinical implications in the treatment of bone

Table 2
Biodegradation of ceramic in μ-CT

Independent variable	Subgroup	Mean value ± SD (remaining ceramic/total ceramic volume in %)	*n*	Post-hoc comparison[a]	*p* value[b]/df/*z* value
Bio degradation of ceramic in μ-CT	CDHA only	75 ± 8.09	6	a	<0.0005/4/7.869
	CDHA + rabbit MSC	61.83 ± 5.74	6	b	
	CDHA + PRP	57 ± 7.17	5	b	
	CDHA + rabbit MSC + PRP	60.16 ± 7.88	6	b	

[a] Different letters indicate significant differences between homogeneous subgroups at an alpha level of $p < 0.05$.
[b] By ANOVA.

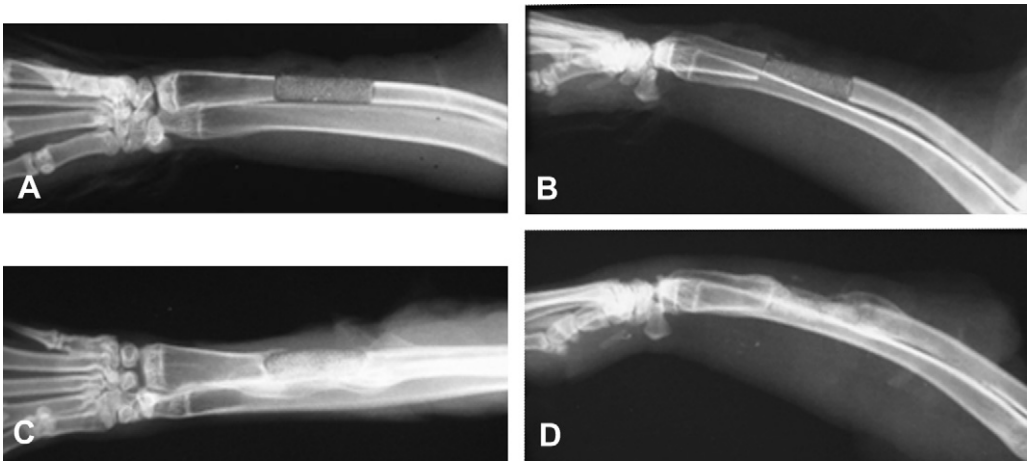

Fig. 5. Anteroposterior (A) and lateral (B) radiographs show a ceramic + PRP + MSC implant postoperatively. Sixteen weeks after implantation a strong biologic reaction with bone formation is visible in AP (C) and lateral (D) views.

defects. Allogenic PRP could be freezed, stored and used in trauma cases for patients who are at a higher risk of non-unions (e.g. smokers) or in patients with osteoporosis who have a reduced bone stock. PRP could be applied into the bone defects and this might improve bone healing.

A major concern regarding the scaffold CDHA is the rate of bone formation of 11% in CDHA alone,e.g. 26% in the CDHA + MSC + PRP group. Lousia et al. examined a coral scaffold with MSC in a similar model and found bone formation with MSC of 30% (SD 13) and 8% (SD 8) with the coral alone in histomorphometry [48]. Geiger et al. found bone formation of 28% in coral scaffolds in a rabbit radius defect and an increase up to 60% with the addition of VEGF in μ-CT after 12 weeks [25]. Petite et al. found bone formation in a sheep metatarsal defect in histomorphometry after 16 weeks using a coral scaffold with medullary bone in an extend of 23% (SD 13) and of 13% (SD 14) for cortical bone [4]. After the addition of 1×10^7 MSC the medullary bone surface area decreased to 17% (SD 6.8) and the cortical one increased up to 54% (SD 11). In the current study the rate of bone formation was on the lower side as well in the empty scaffolds as in the groups with MSC and/or PRP. This might be related to: (i) the PRP (as mentioned above); (ii) the number of MSC; (iii) the scaffold itself; and (iv) the way of measuring bone formation: (ad ii) the number of MSC (5×10^6) was comparable to other studies and the ability to differentiate towards bone was demonstrated in vitro [48,49]. Therefore, we do not think that the number or quality of MSC was inferior. (ad iii) The scaffold CDHA proved to have more favorable properties for bone regeneration than β-tricalcium phosphates after ectopic implantation [7,43], but it might be inferior to coral scaffolds [48]. Future studies should evaluate the scaffolds in the same experiment for better comparison. (ad iv) Furthermore, the method of measurement of bone formation has to be taken into account. It can be influenced by the examiner and the method, e.g. the set of threshold for the identification of bone. It is useful, if different methods are used in the same experiment, e.g.

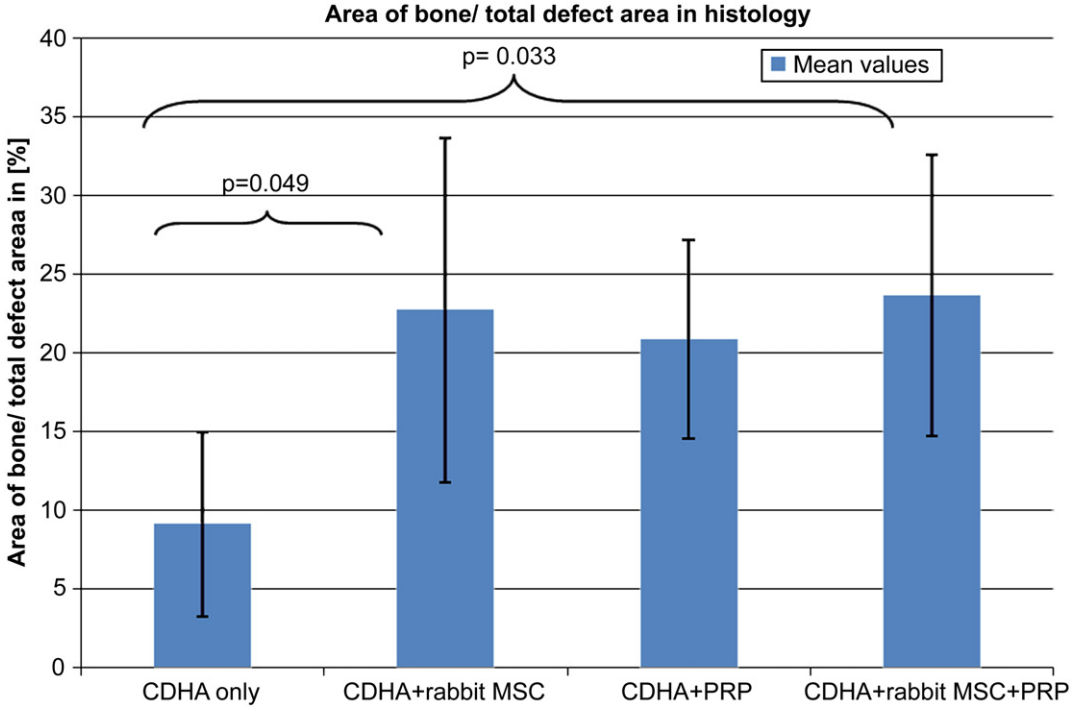

Fig. 6. In histology, the area of newly formed bone was higher in defects treated with CDHA + MSC and with CDHA + MSC + PRP than in defects treated with CDHA alone ($p < 0.05$). Mean values and SD are presented. The numbers were $n = 5$ in the CHDA + PRP group, and $n = 6$ in the other groups.

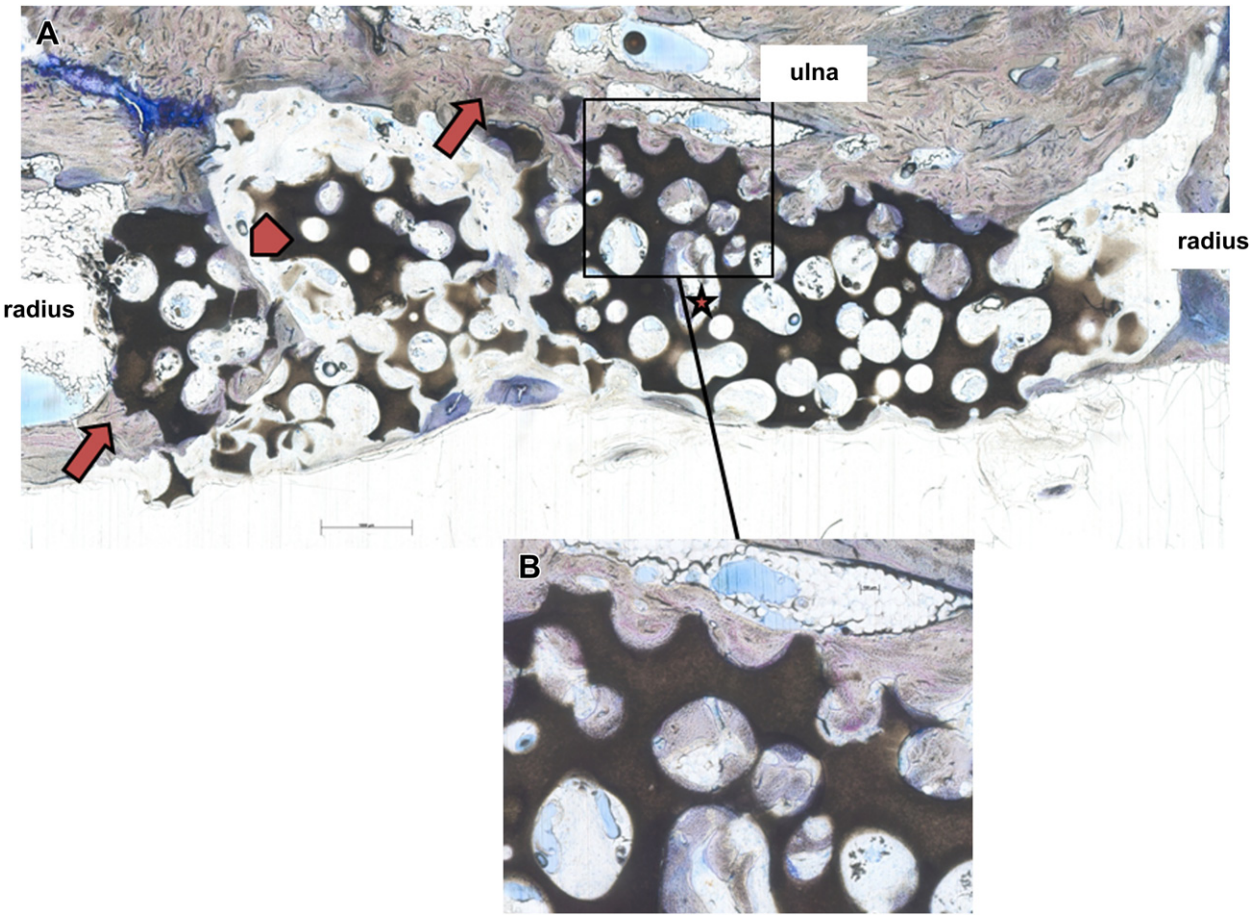

Fig. 7. (A) This CDHA + PRP + MSC Giemsa/toluidine staining histology slide demonstrates excellent osseous integration of the ceramic into the adjacent ulna and radius (arrows) at 10× magnification. Cracks have developed within the ceramic that has been filled with bone (arrowhead). Bone can also be found in the deeper layers of the ceramic (star). (B) The osteoblasts grow directly on and within the pores of the scaffold as seen at 40× magnification.

the combination of the three-dimensional measurement by μ-CT and a two-dimensional analysis in histology as it was done in the current experiment.

Another parameter that can influence bone formation is the rate of resorption of the scaffold: a coral scaffold is resorbed more rapidly than CDHA. If the scaffold is rapidly resorbed, there is more space to form bone. However, if the scaffold is resorbed too fast, an inflammatory reaction can occur and the biomechanical stability is decreased. There is no consensus about the optimal resorption rate for bone regeneration.

The present study examined not only bone formation in general, but also bone formation at particular sites and the resorption of the scaffold. Firstly, bone formation was higher in areas that were adjacent to bone resection areas and the intact ulna. This underlines the fact that intact cells from the surrounding tissues are crucial for a biologic response to MSC and/or growth factors. Secondly, the resorption of the scaffold was increased by the addition of PRP, MSC or both. This emphasizes the importance of the addition of bioactive ingredients such as growth factors and/or MSC if remodeling of the defect site is the goal of the procedure. Growth factors and MSC can attract other progenitor cells or osteoclasts, and therefore initiate bone remodeling [10,18]. In orthopedic surgery, differences of elasticity in a long-bone create sites of increased risk for fracture. Therefore, it seems favorable if the scaffold is resorbed sooner than later, but at the same speed as new bone forms, to achieve a remodeled bone with homogeneous elasticity.

It might be argued that the use of allogenic and pooled PRP is a limitation and falsification of the experimental design and the clinical reality. However, the use of allogenic and pooled PRP was an attempt to standardize the quality of PRP. This reduces the variability and might lead to better results than could be achieved by using an individual's PRP. The application of allogenic PRP did not cause immunologic reactions clinically or in histology. We are aware of the fact that these methods are not sufficient to completely rule out an immunologic reaction, but make them unlikely. The lack of immunologic reactions after the application of allogenic PRP is in accordance with previous reports of wound and bone healing, this might be related to the fact that platelets do not express immunological relevant surface antigens such as HLA 2 [30,50,51]. The use of allogenic PRP has the advantage of a clinical usage "off-the-shelf" without the autogenous preparation at the site of care. Another limitation is that there was no study group with another growth factor, e.g. bone morphogenic protein-2: a direct comparison would have been interesting to judge the osteogenic potential of PRP. However, the aim of the study was to evaluate the effect of PRP in combination with a high-surface scaffold and MSC, and not to compare it to other kinds of growth factors. This should be addressed in future studies.

5. Conclusion

PRP yielded better bone formation than the empty CDHA scaffold as determined by both histology and micro-computer tomography after 16 weeks, whereas no difference was observed on biomechanical testing. Similar behavior was found in samples

with MSC; however, the combination of MSC and PRP did not further improve bone healing. The addition of MSC to PRP could be omitted in the described rabbit model in the future. Furthermore, the resorption of CDHA was improved by the addition of PRP, MSC and MSC/PRP, but there were no differences between the groups. In conclusion, PRP improves bone healing in a diaphyseal rabbit model on CDHA. This study supports the allogenic use of PRP for bone healing as an off-the-shelf therapy.

Acknowledgements

This study was funded by the Orthopaedic University Hospital Heidelberg. The Dr. h.c. Robert Mathys Foundation supported the study with donation of biomaterials. The authors are grateful to Dr. Beat Gasser and Dr. Marc Bohner, both of the Dr. h.c. Robert Mathys Foundation, for help in designing the study; and to K. Goetzke, and A. Krauthoff for technical assistance with histology. We thank Dr. Moser for the statistical analysis.

References

[1] Arrington ED, Smith WJ, Chambers HG, Bucknell AL, Davino NA. Complications of iliac crest bone graft harvesting. Clin Orthop 1996;329:300–9.
[2] Damien C, Parsons R. Bone graft and bone graft substitutes: review of current technology and applications. J Appl Biomat 1991;2:187–208.
[3] Wiltfang J, Kloss FR, Kessler P, Nkenke E, Schultze-Mosgau S, Zimmermann R, et al. Effects of platelet-rich plasma on bone healing in combination with autogenous bone and bone substitutes in critical-size defects. Clin Oral Implants Res 2004;15(2):187–93.
[4] Petite H, Viateau V, Bensaid W, Meunier A, de Pollak C, Bourguignon M, et al. Tissue-engineered bone regeneration. Nat Biotechnol 2000;18(9):959–63.
[5] Kasten P, Luginbühl R, van Griensven M, Barkhausen T, Krettek C, Bohner M, et al. Comparison of human bone marrow stromal cells seeded on calcium-deficient hydroxyapatite, ß-tricalcium phosphate and demineralized bone matrix. Biomaterials 2003;24(15):2593–603.
[6] Kasten P, Luginbuhl R, Vogel J, Niemeyer P, Weiss S, van Griensven M, et al. [Induction of bone tissue on different biomaterials: an in vitro and a pilot in vivo study in the SCID mouse]. Z Orthop Ihre Grenzgeb 2004;142(4):467–75.
[7] Kasten P, Vogel J, Luginbuhl R, Niemeyer P, Tonak M, Lorenz H, et al. Ectopic bone formation associated with mesenchymal stem cells in a resorbable Calcium deficient hydroxyapatite carrier. Biomaterials 2005;26/29:5879–89.
[8] Prockop DJ. Marrow stromal cells as stem cells for nonhematopoetic tissues. Science 1997;276:71–4.
[9] Quarto R, Mastrogiacomo M, Cancedda R, Kutepov SM, Mukhachev V, Lavroukov A, et al. Repair of large bone defects with the use of autologous bone marrow stromal cells. N Eng J Med 2001;344:385–6.
[10] Bruder SP, Kraus KH, Goldberg VM, Kadiyala S. The effect of implants loaded with autologous mesenchymal stem cells on the healing of canine segmental bone defects. J Bone Joint Surg Am 1998;80(7):985–96.
[11] Bostrom MP, Saleh KJ, Einhorn TA. Osteoinductive growth factors in preclinical fracture and long bone defects models. Orthop Clin North Am 1999;30:647–58.
[12] Kiuru J, Viinikka L, Myllyla G, Personen K, Perheentupa J. Cytoskeleton-dependent release of human platelet epidermal growth factor. Life Sci 1991;49:1997–2003.
[13] Kawase T, Okuda K, Wolff LF, Yoshie H. Platelet-rich plasma-derived fibrin clot formation stimulates collagen synthesis in periodontal ligament and osteoblastic cells in vitro. J Periodontol 2003;74(6):858–64.
[14] Marx RE, Carlson ER, Eichstaedt RM, Schimmele SR, Strauss JE, Georgeff KR. Platelet-rich plasma: growth factor enhancement for bone grafts. Oral Surg Oral Med Oral Pathol Oral Radiol Endod 1998;85(6):638–46.
[15] Choi BH, Im CJ, Huh JY, Suh JJ, Lee SH. Effect of platelet-rich plasma on bone regeneration in autogenous bone graft. Int J Oral Maxillofac Surg 2004;33(1):56–9.
[16] Gandhi A, Dumas C, O'Connor JP, Parsons JR, Lin SS. The effects of local platelet rich plasma delivery on diabetic fracture healing. Bone 2006;38(4):540–6.
[17] Li H, Zou X, Xue Q, Egund N, Lind M, Bunger C. Anterior lumbar interbody fusion with carbon fiber cage loaded with bioceramics and platelet-rich plasma. An experimental study on pigs. Eur Spine J 2004;13(4):354–8.
[18] Roldan JC, Jepsen S, Miller J, Freitag S, Rueger DC, Acil Y, et al. Bone formation in the presence of platelet-rich plasma vs. bone morphogenetic protein-7. Bone 2004;34(1):80–90.
[19] Yamada Y, Ueda M, Naiki T, Takahashi M, Hata K, Nagasaka T. Autogenous injectable bone for regeneration with mesenchymal stem cells and platelet-rich plasma: tissue-engineered bone regeneration. Tissue Eng 2004;10(5–6):955–64.
[20] Bohner M. Calcium orthophosphates in medicine: from ceramics to calcium phosphate cements. Injury 2000;31(Suppl 4):37–47.
[21] LeGeros RZ. Properties of osteoconductive biomaterials: calcium phosphates. Clin Orthop 2002;395(Feb):81–98.
[22] Reyes M, Lund T, Lenvik T, Aguiar D, Koodie L, Verfaillie CM. Purification and ex vivo expansion of postnatal human marrow mesodermal progenitor cells. Blood 2001;98(9):2615–25.
[23] Vogel JP, Szalay K, Geiger F, Kramer M, Richter W, Kasten P. Platelet-rich plasma improves expansion of human mesenchymal stem cells and retains differentiation capacity and in vivo bone formation in calcium phosphate ceramics. Platelets 2006;17(7):462–9.
[24] Wittbjer J, Palmer B, Thorngren KG. Osteogenetic properties of reimplanted decalcified and undecalcified autologous bone in the rabbit radius. Scand J Plast Reconstr Surg 1982;16(3):239–44.
[25] Geiger F, Bertram H, Berger I, Lorenz H, Wall O, Eckhardt C, et al. Vascular endothelial growth factor gene-activated matrix (VEGF165-GAM) enhances osteogenesis and angiogenesis in large segmental bone defects. J Bone Miner Res 2005;20(11):2028–35.
[26] Mattila P, Knuuttila M, Kovanen V, Svanberg M. Improved bone biomechanical properties in rats after oral xylitol administration. Calcif Tissue Int 1999;64(4):340–4.
[27] Reddy GK, Stehno-Bittel L, Hamade S, Enwemeka CS. The biomechanical integrity of bone in experimental diabetes. Diabetes Res Clin Pract 2001;54(1):1–8.
[28] Abramoff MD, Magelhaes PJ, Ram SJ. Image processing with Image J. Biophotonics Int 2004;11(7):36–42.
[29] Kovacs K, Velich N, Huszar T, Szabo G, Semjen G, Reiczigel J, et al. Comparative study of beta-tricalcium phosphate mixed with platelet-rich plasma versus beta-tricalcium phosphate, a bone substitute material in dentistry. Acta Vet Hung 2003;51(4):475–84.
[30] Fuerst G, Gruber R, Tangl S, Sanroman F, Watzek G. Enhanced bone-to-implant contact by platelet-released growth factors in mandibular cortical bone: a histomorphometric study in minipigs. Int J Oral Maxillofac Implants 2003;18(5):685–90.
[31] Graziani F, Ivanovski S, Cei S, Ducci F, Tonetti M, Gabriele M. The in vitro effect of different PRP concentrations on osteoblasts and fibroblasts. Clin Oral Implants Res 2006;17(2):212–9.
[32] Gruber R, Karreth F, Kandler B, Fuerst G, Rot A, Fischer MB, et al. Platelet-released supernatants increase migration and proliferation, and decrease osteogenic differentiation of bone marrow-derived mesenchymal progenitor cells under in vitro conditions. Platelets 2004;15(1):29–35.
[33] Al Sukhun J, Helenius M, Lindqvist C, Thoren H. Use of platelet rich plasma (PRP) in the reconstruction of mandibular bony defects: clinical and radiographic follow-up. Br J Oral Maxillofac Surg 2007 Jan 6 [Epub ahead of print].
[34] Dugrillon A, Klüter H. Topical application of platelets for improved wound healing. Blood Ther Med 2002;3(1):21–6.
[35] Fennis JP, Stoelinga PJ, Jansen JA. Mandibular reconstruction: a histological and histomorphometric study on the use of autogenous scaffolds, particulate cortico-cancellous bone grafts and platelet rich plasma in goats. Int J Oral Maxillofac Surg 2004;33(1):48–55.
[36] Akca K, Cehreli M, Demiralp B, Guzel E, Dagdeviren A. Platelet-rich plasma and bone healing: a histologic study in titanium bone chambers. Int J Periodontics Restorative Dent 2007;27(4):387–92.
[37] Aghaloo TL, Moy PK, Freymiller EG. Evaluation of platelet-rich plasma in combination with anorganic bovine bone in the rabbit cranium: a pilot study. Int J Oral Maxillofac Implants 2004;19(1):59–65.
[38] Mooren RE, Merkx MA, Bronkhorst EM, Jansen JA, Stoelinga PJ. The effect of platelet-rich plasma on early and late bone healing: an experimental study in goats. Int J Oral Maxillofac Surg 2007;36(7):626–31.
[39] You TM, Choi BH, Li J, Jung JH, Lee HJ, Lee SH, et al. The effect of platelet-rich plasma on bone healing around implants placed in bone defects treated with Bio-Oss: a pilot study in the dog tibia. Oral Surg Oral Med Oral Pathol Oral Radiol Endod 2007;103(4):e8–12.
[40] Vasconcelos Gurgel BC, Goncalves PF, Pimentel SP, Ambrosano GM, Nociti Junior FH, Sallum EA, et al. Platelet-rich plasma may not provide any additional effect when associated with guided bone regeneration around dental implants in dogs. Clin Oral Implants Res 2007;18(5):649–54.
[41] Plachokova AS, van den Dolder J, Stoelinga PJ, Jansen JA. Early effect of platelet-rich plasma on bone healing in combination with an osteoconductive material in rat cranial defects. Clin Oral Implants Res 2007;18(2):244–51.
[42] Thor A, Franke-Stenport V, Johansson CB, Rasmusson L. Early bone formation in human bone grafts treated with platelet-rich plasma: preliminary histomorphometric results. Int J Oral Maxillofac Surg 2007;36(12):1164–71.
[43] Kasten P, Vogel J, Luginbuhl R, Niemeyer P, Weiss S, Schneider S, et al. Influence of platelet-rich plasma on osteogenic differentiation of mesenchymal stem cells and ectopic bone formation in calcium phosphate ceramics. Cells Tissues Organs 2006;183(2):68–79.
[44] Weibrich G, Kleis WK, Hafner G, Hitzler WE, Wagner W. Comparison of platelet, leukocyte, and growth factor levels in point-of-care platelet-enriched plasma, prepared using a modified Curasan kit, with preparations received from a local blood bank. Clin Oral Implants Res 2003;14(3):357–62.
[45] van den Dolder J, Mooren R, Vloon AP, Stoelinga PJ, Jansen JA. Platelet-rich plasma: quantification of growth factor levels and the effect on growth and differentiation of rat bone marrow cells. Tissue Eng 2006;12(11):3067–73.
[46] Weibrich G, Gnoth SH, Otto M, Reichert TE, Wagner W. [Growth stimulation of human osteoblast-like cells by thrombocyte concentrates in vitro]. Mund Kiefer Gesichtschir 2002;6(3):168–74.

[47] Lieberman JR, Daluiski A, Einhorn TA. The role of growth factors in the repair of bone. Biology and clinical applications. J Bone Joint Surg Am 2002;84-A(6):1032–44.
[48] Louisia S, Stromboni M, Meunier A, Sedel L, Petite H. Coral grafting supplemented with bone marrow. J Bone Joint Surg Br 1999;81(4):719–24.
[49] Geiger F, Lorenz H, Xu W, Szalay K, Kasten P, Claes L, et al. VEGF producing bone marrow stromal cells (BMSC) enhance vascularization and resorption of a natural coral bone substitute. Bone 2007;41(4):516–22.
[50] Pietramaggiori G, Scherer SS, Mathews JC, Alperovich M, Yang HJ, Neuwalder J, et al. Healing modulation induced by freeze-dried platelet-rich plasma and micronized allogenic dermis in a diabetic wound model. Wound Repair Regen 2008;16(2):218–25.
[51] Pietramaggiori G, Kaipainen A, Czeczuga JM, Wagner CT, Orgill DP, Fuerst G, et al. Freeze-dried platelet-rich plasma shows beneficial healing properties in chronic wounds. Wound Repair Regen 2006;14(5):573–80.